

Critical layer thickness in strained $\text{Ga}_{1-x}\text{In}_x\text{As}/\text{InP}$ quantum wells

Cite as: Appl. Phys. Lett. 55, 1668 (1989); <https://doi.org/10.1063/1.102231>

Submitted: 11 May 1989 • Accepted: 13 August 1989 • Published Online: 04 June 1998

H. Temkin, D. G. Gershoni, S. N. G. Chu, et al.



View Online



Export Citation

ARTICLES YOU MAY BE INTERESTED IN

[Calculation of critical layer thickness versus lattice mismatch for \$\text{Ge}_x\text{Si}_{1-x}/\text{Si}\$ strained-layer heterostructures](#)

Applied Physics Letters **47**, 322 (1985); <https://doi.org/10.1063/1.96206>

[Band parameters for III-V compound semiconductors and their alloys](#)

Journal of Applied Physics **89**, 5815 (2001); <https://doi.org/10.1063/1.1368156>

[Critical thicknesses of highly strained InGaAs layers grown on InP by molecular beam epitaxy](#)

Applied Physics Letters **60**, 2249 (1992); <https://doi.org/10.1063/1.107045>

Lock-in Amplifiers
up to 600 MHz



Zurich
Instruments



Critical layer thickness in strained $\text{Ga}_{1-x}\text{In}_x\text{As}/\text{InP}$ quantum wells

H. Temkin, D. G. Gershoni, S. N. G. Chu, J. M. Vandenberg, R. A. Hamm, and M. B. Panish

AT&T Bell Laboratories, Murray Hill, New Jersey 07974

(Received 11 May 1989; accepted for publication 13 August 1989)

We use a combination of electrical, optical, and structural characterization techniques to determine the critical layer thickness of strained $\text{Ga}_{1-x}\text{In}_x\text{As}/\text{InP}$ quantum wells. Well compositions covering the entire range of strain available, from -3.8% (GaAs) to $+3.2\%$ (InAs), were investigated. We find that the critical layer thickness in this material system is unambiguously described by the classical Matthews and Blakeslee force balance model [J. Cryst. Growth 27, 118 (1974)]. Reverse leakage current of strained-well samples grown in a $p-i-n$ configuration is shown to be the most direct and reliable measure of the pseudomorphic limit.

In recent years, much attention has been given to strained-layer superlattices (SLS), in which multilayer structures are grown lattice mismatched to the substrate but with the layer thickness small enough to accommodate the mismatch strain coherently rather than by misfit dislocations. The elastic layer strain gives rise to a number of interesting properties and SLSs can be conveniently used to study strain effects. We have shown previously that the normally lattice-matched $\text{Ga}_{1-x}\text{In}_x\text{As}$ grown on InP is in many ways an ideal system to study the effect of strain on the electronic and optical properties of quantum wells.¹⁻⁶ The critical layer thickness above which pseudomorphic growth cannot be supported in this material system has not yet been determined. Previous attempts at establishing the critical layer thickness in other material systems, such as $\text{Ga}_{1-x}\text{In}_x\text{As}/\text{GaAs}$ (Refs. 7-9) and $\text{Ge}_x\text{Si}_{1-x}/\text{Si}$ (Ref. 10), have turned out to be quite difficult and even controversial. The question is important for the understanding of the origin of defects through which the strain relaxation occurs and in most device applications of strained layers.

In this letter we study the critical layer thickness (d_c) of $\text{Ga}_{1-x}\text{In}_x\text{As}$ grown on InP. Quantum well samples were grown by gas source molecular beam epitaxy covering the entire range of In concentrations x from GaAs ($x = 0$) to InAs ($x = 1$). The samples were extensively characterized by electrical, optical, and structural (transmission electron microscopy and high-resolution x-ray diffraction) measurements. We show that the electrical measurements, not used for this purpose previously, are particularly sensitive to the onset of strain-related defects. The quality of $p-n$ junction devices based on strained layers is of course a final measure of the SLS quality in most device applications. Our results clearly demonstrate that the critical layer thickness of $\text{Ga}_{1-x}\text{In}_x\text{As}/\text{InP}$ is limited by the conservative Matthews and Blakeslee force balance model.¹¹

SLS wafers were grown at 500°C on (100) oriented n -InP substrates, on which a $0.25\text{-}\mu\text{m}$ -thick InP buffer layer was deposited prior to the superlattice. Two sets of SLS samples were prepared. The first set consisted of five identical quantum wells separated by $300\text{-}\text{\AA}$ -thick barriers. The well composition was kept at $x = 0.32$ and 0.74 in different samples. The well widths were 40, 60, 100, and 160 \AA , again in different samples, in order to establish the critical layer thickness at each composition. In the second set of 14 sam-

ples the superlattice region consisted of ten $\text{In}_x\text{Ga}_{1-x}\text{As}$ wells, with the thicknesses close to the critical limit estimated from the Matthews-Blakeslee model.¹¹ The number of wells, their widths, and the widths of InP barriers were chosen to assure that the critical thickness of the entire superlattice was below the critical limit. The concentration of In in these structures was varied from $x = 0$ to 1.0, resulting in four samples with lattice constant larger than that of the substrate, i.e., subjected to compressive biaxial stress, and the remaining eight under tension. The strained wells were separated by InP barriers ranging in thickness from 250 to 400 \AA in different samples. In all the samples the superlattice regions were capped with a $1000\text{-}\text{\AA}$ -thick undoped n -InP layer, followed by a $3000\text{-}\text{\AA}$ -thick layer of InP doped p type with Be. The SLS structure thus comprised the i layer of a $p-i-n$ diode. While the junction was misplaced in each case into InP, the SLS structure was well within the depletion region even at very low reverse bias voltages. Electrical measurements were carried out on $100\text{-}\mu\text{m}$ -diam mesa diodes defined by wet etching.

The well dimensions and compositions were determined from transmission electron microscope (TEM) cross sections and high-resolution x-ray diffraction (HRXRD). A TEM cross section of a SLS structure with $160\text{-}\text{\AA}$ -thick wells of $x = 0.37$ composition is shown in Fig. 1. The (200) reflection shows very well defined quantum wells. The lattice mismatch strain is accommodated elastically, as revealed by strong (400) reflection contrast. Defects of the type shown in Fig. 1 can be seen in the bottom or top SLS interfaces. The resulting slip plane is observed in all the wells. Occasionally, stacking faults along the $\{111\}$ planes, which propagate through the entire structure, are also observed. Their density is estimated at less than $4 \times 10^8\text{ cm}^{-2}$. Similar defect structures are observed in the $x = 0.75$ sample with 160 \AA wells, subjected to compressive strain. The difference in defect type with the sign of strain is of interest for the determination of the slip mechanism for the misfit generation.¹² In general, TEM cross sections do not show defects in less strained SLSs. It is well known that TEM, which images only very small areas, is not sensitive to low defect densities. For instance, the lattice mismatch strain in the 100 \AA well, $x = 0.37$, sample is apparently just large enough to produce misfit dislocations. A low density (less than $30\text{-}50\text{ cm}^{-1}$) of misfit lines lying only in one of the (110) directions can be

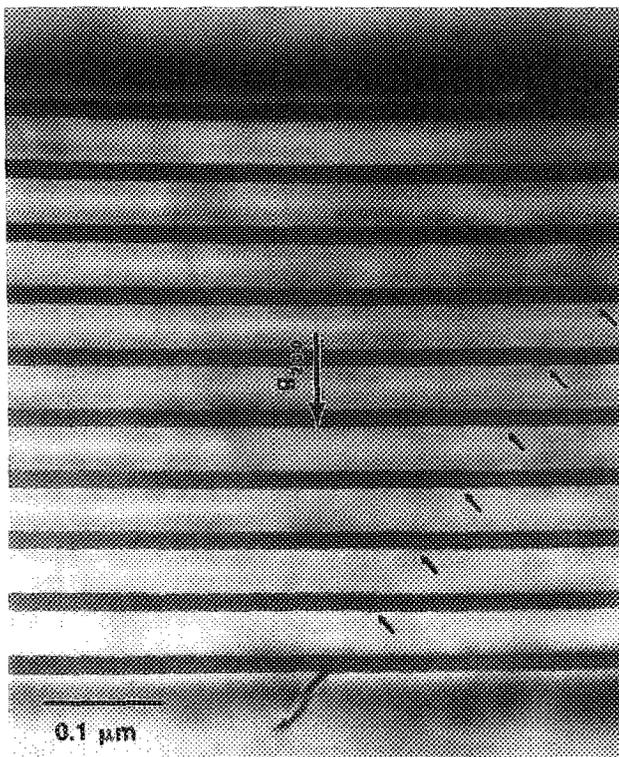


FIG. 1. TEM cross section of a SLS structure. Wells are 160 Å thick and composition of $x = 0.3$ was determined by HRXRD fitting. Arrows indicate a slip plane propagation through the SLS. Defects are not observed in thinner well SLS structures of this composition.

seen in the Nomarski contrast optical microscope. These defects were not observed in the TEM samples prepared from this wafer.

The strain component parallel to the growth direction and the In concentrations were determined by fitting the HRXRD spectra with a kinematic diffraction model described previously.¹³ This procedure determines the In concentration with precision better than 1%. Most of the SLS structures show very well resolved (400) superlattice spectra. The sharpness and intensity of the satellite reflections are indicative of very high sample quality, as defined by the interface sharpness and planarity in the growth direction. Similar quality spectra were obtained from SLS samples spanning the entire range of well thicknesses studied, for a fixed composition, as well as most of the samples spanning the range of In concentrations. Superlattice diffraction satellite spectra could not be obtained only for structures with $x < 0.1$ in which strain-induced slip line density, as judged from TEM cross sections, exceeded $6 \times 10^9 \text{ cm}^{-2}$.

Room-temperature photoluminescence (PL) spectra of a set of SLS structures with $x = 0.37$ and 0.75 are shown in Fig. 2. The spectra span a wide spectral range, from 1.3 to nearly $2 \mu\text{m}$. The PL linewidth does not vary with composition when plotted on the energy scale, indicating a high degree of compositional uniformity. The high luminescence efficiency does not degrade significantly with increasing strain. The changes in the band gap with composition and strain result in large shifts from the lattice-matched wavelength of $1.66 \mu\text{m}$. In addition, the quantum size effect results in a considerable blue shift of the PL peak with decrease-

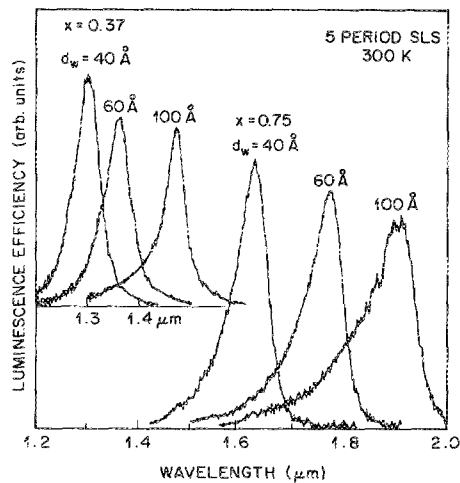


FIG. 2. Room-temperature photoluminescence spectra of two sets of SLS samples with $x = 0.37$ and $x = 0.75$, respectively. Well thickness was varied from 40 to 100 Å.

ing well thickness. For instance, the luminescence of the In-rich SLS shifts from ~ 2 to $1.62 \mu\text{m}$ as the well width is reduced from 100 to 40 Å. The exciton energies seen in the PL spectra are identified as the $n = 1$ electron-light hole (for the $x = 0.37$ set) and heavy hole (for $x = 0.75$) transitions. For compositions corresponding to $x < 0.44$, the heavy and light hole transitions switch positions and the light hole level becomes the lowest energy state.¹ The energies of light hole excitons of the $x = 0.37$ set are in excellent agreement, to within 5 meV, with the values calculated on the basis of a phenomenological deformation potential model described previously.^{1,2} This includes the sample with 160-Å-wide wells, not illustrated in Fig. 2. The energies of In-rich SLS samples in this set are typically ~ 20 – 25 meV lower than the calculated values. This Stokes shift is also seen in lattice-matched wells and has been discussed previously.⁶ The good agreement between the measured and calculated excitonic transition energies⁵ would imply that strain in the wells is accommodated elastically and all of these structures are pseudomorphic. However, such a conclusion is not justified since an appreciable amount of strain relief can take place before it could be detected by optical measurements. For instance, the linear density of dislocations induced in the thicker well samples, on the order of $2 \times 10^4/\text{cm}$ as shown in Fig. 1, relaxes the elastic strain no more than 4%.¹⁴ This is not sufficient to affect the optical measurements. However, the dislocation density is sufficient to degrade the electrical characteristics of SLS-based diodes, as discussed below. Problems with the use of simple PL measurements, and advantages of PL microscopy, for the purpose of determining the critical layer thickness have been discussed previously.⁹ Despite this, the use of PL remains quite popular¹⁵ due perhaps to the ease of use and general availability of the technique.

The reverse leakage characteristics of the 100- μm -diam mesa diodes fabricated from the $x = 0.37$ samples are shown in Fig. 3. The SLS samples with the well dimensions of 40 and 60 Å show very well behaved current-voltage (I - V) characteristics. The reverse currents saturate at very low levels, less than 1 nA up to 10 V, and are very reproducible. Ten

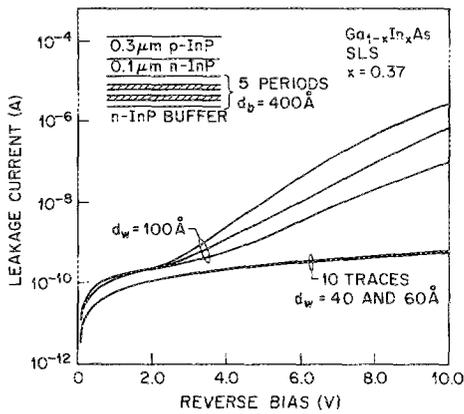


FIG. 3. Reverse leakage currents measured as a function of bias for *p-i-n* diodes in which the *i* layer consists of a five-period superlattice. Well thicknesses were varied in different structures of the same well composition.

traces plotted here for these diodes are virtually identical. These *I-V* characteristics are also indistinguishable from those of the control samples grown without a superlattice in the *i* region. The *I-V* characteristics of the 100 Å well sample are much worse. The leakage currents increase by as much as four orders of magnitude at 10 V, and the results are not reproducible. The breakdown voltage decreases from 30–35 to ~15 V. The same results were obtained on devices with $x = 0.75$ SLS composition. The two sets of diodes (not shown) fabricated from the 160 Å SLS wafers exhibit even poorer characteristics. In general, as established by similar experiments on diodes with a range of In concentrations, the *I-V* characteristics do not degrade for SLS thicknesses below and up to the critical thickness. In contrast, the *I-V* characteristics degrade sharply for larger SLS dimensions.

It should be stressed that the above comments apply specifically to *p-i-n* diodes of the type illustrated in Fig. 3, in which the depletion front moves through the SLS region under reverse bias. It is possible to mask the effect of strain-induced defects by doping the SLS much higher than the adjacent, and oppositely doped, bulk layer. In such an abrupt diode, an example of which could be the base-collector junction of a bipolar transistor, the depletion layer will be contained mostly to the defect-free, low-doped cladding layer. Experiments carried out on such diodes in the $\text{Ge}_x\text{Si}_{1-x}/\text{Si}$ system show high junction quality for SLS thicknesses as much as a factor of 2 larger than d_c .¹⁶

Figure 1 shows a plot of the critical layer thickness of $\text{Ga}_{1-x}\text{In}_x\text{As}$ as a function of In concentration. Pseudomorphic samples, i.e., those largely free of strain-induced defects, are shown as open circles. Samples which have relaxed, as judged by the *p-n* junction quality, are labeled by filled circles. The solid curves represent the critical thicknesses calculated on the basis of force balance (FB) model proposed by Matthews and Blakeslee,¹¹ and the energy balance (EB) model of People and Bean.¹⁰ The elastic parameters used in the calculation were obtained from the compilations of Adachi.¹⁷ The application of the first model to III-V alloy systems such as $\text{Ga}_{1-x}\text{In}_x\text{As}/\text{GaAs}$ appears to be now well justified.⁹ Its validity has, however, been repeatedly challenged on the basis of low-resolution x-ray diffraction and photoluminescence measurements.^{8,15} The latter model has

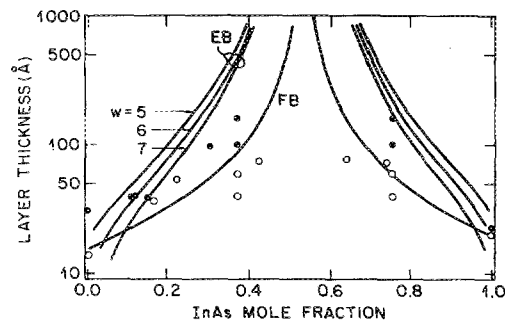


FIG. 4. Strained-layer thickness plotted as a function of the In concentration x . Lines represent the critical layer thickness of $\text{Ga}_{1-x}\text{In}_x\text{As}/\text{InP}$ calculated from the models of Matthews and Blakeslee and People and Bean.

been first applied to the $\text{Ge}_x\text{Si}_{1-x}/\text{Si}$ system using a fitting parameter w , loosely defined as the width of an isolated dislocation, of approximately five (110) atomic spacings. The EB curves plotted in Fig. 4 use $w = 5, 6,$ and 7 . The quantum well thickness limits of the two models differ by as much as two orders of magnitude for low values of the lattice-mismatch strain, close to $x = 0.53$ in the present case, and factors of 2 in the limits of $x = 0$ and 1. The samples which exceed the critical thickness of the FB model show partially relaxed superlattices. The data of Fig. 4 conclusively show that the critical layer thicknesses of $\text{Ga}_{1-x}\text{In}_x\text{As}/\text{InP}$ are determined by the Matthews and Blakeslee equilibrium force balance model. We find it is not possible to exceed the critical thickness and maintain high electrical quality of the SLS contained in the depletion region, under the compressive and tensile strain conditions alike. While the critical layer thickness might be, to some degree, affected by the detailed growth conditions, we have not been able to alter the limit in a wide range of samples grown. It must be presumed that the failure of *p-i-n*'s that exceed the critical thickness results from additional defects over and above the 10^3 – 10^4 cm^{-2} threading dislocations arising from the substrate.

- ¹D. Gershoni, J. M. Vandenberg, R. A. Hamm, H. Temkin, and M. B. Panish, *Phys. Rev. B* **36**, 1320 (1987).
- ²D. Gershoni, H. Temkin, J. M. Vandenberg, S. N. G. Chu, R. A. Hamm, and M. B. Panish, *Phys. Rev. Lett.* **60**, 448 (1988).
- ³D. Gershoni, H. Temkin, and M. B. Panish, *Appl. Phys. Lett.* **53**, 1294 (1988).
- ⁴R. People, *Appl. Phys. Lett.* **50**, 1604 (1987).
- ⁵D. Gershoni, H. Temkin, and M. B. Panish, *Phys. Rev. B* **38**, 7870 (1988).
- ⁶D. Gershoni, H. Temkin, M. B. Panish, and R. A. Hamm, *Phys. Rev. B* **39**, 5531 (1989).
- ⁷I. J. Fritz, S. T. Picraux, L. R. Dawson, T. J. Drummond, W. D. Laidig, and N. G. Anderson, *Appl. Phys. Lett.* **46**, 967 (1985).
- ⁸P. J. Orders and B. F. Usher, *Appl. Phys. Lett.* **50**, 980 (1987).
- ⁹I. J. Fritz, P. L. Gourley, and L. R. Dawson, *Appl. Phys. Lett.* **51**, 1004 (1987).
- ¹⁰R. People and J. C. Bean, *Appl. Phys. Lett.* **47**, 322 (1985).
- ¹¹J. W. Matthews and A. E. Blakeslee, *J. Cryst. Growth* **27**, 118 (1974).
- ¹²P. M. J. Maree, J. C. Barbour, J. F. van der Veen, K. L. Kavanagh, C. W. T. Bulle-Lieuwma, and M. P. A. Vieggers, *J. Appl. Phys.* **62**, 4413 (1987).
- ¹³J. M. Vandenberg, R. A. Hamm, M. B. Panish, and H. Temkin, *J. Appl. Phys.* **62**, 1278 (1987).
- ¹⁴S. N. G. Chu, A. T. Macrander, K. Stregge, and W. D. Johnston, Jr., *J. Appl. Phys.* **57**, 249 (1985).
- ¹⁵J. P. Reithmaier, H. Cerva, and R. Losch, *Appl. Phys. Lett.* **54**, 48 (1989).
- ¹⁶C. A. King, J. L. Hoyt, C. M. Gronet, J. F. Gibbons, and S. D. Wilson, *IEEE Electron Device Lett.* **9**, 229 (1988).
- ¹⁷S. Adachi, *J. Appl. Phys.* **53**, 8775 (1982).